

Luminescence properties of $\text{NaGd}(\text{PO}_3)_4:\text{Eu}^{3+}$ and energy transfer from Gd^{3+} to Eu^{3+}

J. Zhong · H. Liang · Q. Su · J. Zhou · Y. Huang ·
Z. Gao · Y. Tao · J. Wang

Received: 20 April 2009 / Revised version: 27 May 2009 / Published online: 6 August 2009
© Springer-Verlag 2009

Abstract The luminescence properties of polyphosphates $\text{NaEu}_x\text{Gd}_{(1-x)}(\text{PO}_3)_4$ ($x = 0-1.00$) and the energy transfer from Gd^{3+} to Eu^{3+} were studied. In undoped $\text{NaGd}(\text{PO}_3)_4$ sample, the photon cascade emission of Gd^{3+} was observed under $^8\text{S}_{7/2} \rightarrow ^6\text{G}_J$ excitation (201 nm) in which the emission of a red photon due to $^6\text{G}_J \rightarrow ^6\text{P}_J$ transition is followed by an ultraviolet photon emission due to $^6\text{P}_J \rightarrow ^8\text{S}_{7/2}$ transition. When part of Gd^{3+} ions in the host $\text{NaGd}(\text{PO}_3)_4$ were substituted by Eu^{3+} ions, the $\text{NaGd}(\text{PO}_3)_4:\text{Eu}^{3+}$ sample showed intensive red emission under 172-nm vacuum-ultraviolet (VUV) excitation which is suitable for mercury-free fluorescent lamps and plasma display panel applications. Based on the VUV-visible spectroscopic characteristics and the luminescence decay properties of $\text{NaGd}(\text{PO}_3)_4:\text{Eu}^{3+}$, it was found that the quantum cutting by a two-step energy transfer from Gd^{3+} to Eu^{3+} can improve the red emission of Eu^{3+} ions under VUV excitation but only a part of the excitation energy in the excited $^6\text{P}_J$ states within Gd^{3+} ions can be transferred to Eu^{3+} ions

for its red emission, and the nonradiative energy transfer efficiencies from the excited $^6\text{P}_J$ states within Gd^{3+} to Eu^{3+} were calculated.

PACS 78.55.-m · 42.70.-a · 78.20.-e

1 Introduction

The oxide phosphors doped with Eu^{3+} ions have received great concern due to their good photoluminescence characteristics. They are often used as red-emitting phosphors in the fields of lighting and displaying under the excitation of ultraviolet (UV) or vacuum-ultraviolet (VUV) light. For example, $(\text{Y}, \text{Gd})\text{BO}_3:\text{Eu}^{3+}$ is a well-known red-emitting phosphor for mercury-free fluorescent tubes and plasma display panels (PDPs) because of its high luminous efficiency under VUV excitation.

In both mercury-free fluorescent tubes and PDPs application, the VUV radiation generated by a noble gas discharge is used as the excitation source, which is converted into visible light by the VUV phosphors. But the energy of a VUV photon is more than twice the energy of a visible photon. If a VUV photon is converted into a visible photon, the energy efficiency will be much lower. Trivalent gadolinium ion (Gd^{3+}) doped in LiYF_4 can give a photon cascade emission (quantum cutting) upon $^8\text{S}_{7/2} \rightarrow ^6\text{G}_J$ excitation [1], that is after absorbing a high-energy VUV photon Gd^{3+} ion acting as a quantum cutter can emit a red photon due to the $^6\text{G}_J \rightarrow ^6\text{P}_J$ transition and an ultraviolet photon due to the $^6\text{P}_J \rightarrow ^8\text{S}_{7/2}$ transition. And the energy of both transitions can be transferred to Eu^{3+} ions through a two-step energy transfer for emitting two red photons, so a visible quantum efficiency of 190% from a VUV photon can be obtained [2, 3]. So an efficient energy transfer from the donor to the acceptor is a

J. Zhong · H. Liang (✉) · Q. Su · J. Zhou
State Key Laboratory of Optoelectronic Materials and
Technologies, MOE Laboratory of Bioinorganic and Synthetic
Chemistry, School of Chemistry and Chemical Engineering,
Sun Yat-sen University, Guangzhou 510275,
People's Republic of China
e-mail: cesbin@mail.sysu.edu.cn
Fax: +86-20-84111038

Y. Huang · Z. Gao · Y. Tao
Laboratory of Beijing Synchrotron Radiation, Institute of High
Energy Physics, Chinese Academy of Science, Beijing 100039,
People's Republic of China

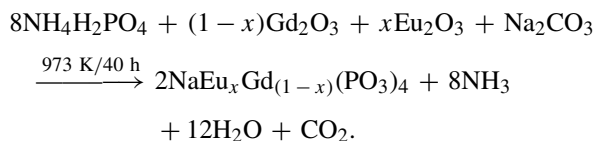
J. Wang
State Key Laboratory of Crystal Material, Shandong University,
Jinan 250100, People's Republic of China

critical requirement to yield a high luminous efficiency for the visible emission under VUV excitation.

The inorganic condensed polyphosphates with general formula $M^I\text{RE}^{\text{III}}(\text{PO}_3)_4$ (where M^I are alkali metal ions and RE^{III} are rare-earth metal ions) are relatively stable under ambient conditions of temperature and humidity [4, 5]. These compounds can be kept for many years in a perfect state of crystallinity and they are not water soluble [6]. They have been extensively investigated in the past years due to their interesting optical properties [7–9]. In our recent works, the intensive green and white emission were obtained when trivalent terbium ion (Tb^{3+}) and dysprosium (Dy^{3+}) were doped in the polyphosphate $\text{NaGd}(\text{PO}_3)_4$, respectively [10, 11]. In order to obtain a new red-emitting VUV phosphor, Eu^{3+} -activated $\text{NaGd}(\text{PO}_3)_4$ ($\text{NaGd}(\text{PO}_3)_4:\text{Eu}^{3+}$) powder samples were prepared in the present work. After the photon cascade emission of Gd^{3+} in $\text{NaGd}(\text{PO}_3)_4$ was determined, the intensive red emission of $\text{NaGd}(\text{PO}_3)_4:\text{Eu}^{3+}$ was measured under 172-nm VUV excitation, because the 172-nm VUV photon is one of the maximum wavelengths yielded by the xenon dimmer discharge. And the energy transfer behaviors from Gd^{3+} to Eu^{3+} ions were analyzed according to the spectroscopic characteristics and the luminescence decay properties of $\text{NaGd}(\text{PO}_3)_4:\text{Eu}^{3+}$.

2 Experimental details

A series of polycrystalline samples of $\text{NaEu}_x\text{Gd}_{(1-x)}(\text{PO}_3)_4$ ($x = 0-1.00$) were synthesized by a high-temperature solid-state reaction of stoichiometric amounts ($\text{Na}/\text{RE}/\text{P} = 1:1:4$) of analytical reagent grade Na_2CO_3 , $\text{NH}_4\text{H}_2\text{PO}_4$, and 99.99% pure rare-earth oxides (Gd_2O_3 and Eu_2O_3) using the following reactions:



The pulverous mixtures were ground in an agate mortar and then calcinated at 973 K (700°C) for 40 h in a corundum crucible under air atmosphere.

The X-ray powder diffraction analyses were carried out with a Rigaku D/max 2200 vpc X-ray powder diffractometer (Cu $K\alpha$ radiation, 40 kV, 30 mA) at room temperature (RT), and the data were collected with $2\theta = 10-60^\circ$, step size = 0.02° .

The UV luminescence spectra and luminescence decay curves at RT were recorded on an Edinburgh FLS 920 combined fluorescence lifetime and steady state spectrometer, which was equipped with a time-correlated single-photon counting (TCSPC) card. A 450-W xenon lamp was used as the excitation source for the UV-visible spectra and a blue-

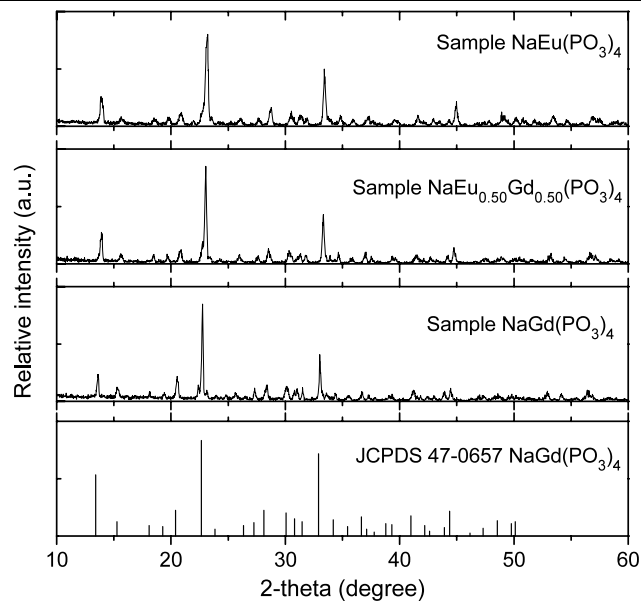


Fig. 1 XRD patterns of samples $\text{NaGd}(\text{PO}_3)_4$, $\text{NaEu}_{0.05}\text{Gd}_{0.95}(\text{PO}_3)_4$, and $\text{NaEu}(\text{PO}_3)_4$

sensitive photomultiplier tube (R1527 PMT) was used for the emission spectra recording. The excitation photons for the luminescence decay curve determining were provided by a 60-W μF flash lamp with pulse width of 1.5–3.0 μs .

The VUV spectra were recorded at Beamline 4B8 in Beijing Synchrotron Radiation Facilities (BSRF) under dedicated synchrotron mode (2.5 GeV, 150–60 mA). A 1 m Seya monochromator (1200 grooves/mm, 120–350 nm, 1-nm bandwidth) was used for the synchrotron radiation excitation spectra measurement, and an Acton SP-308 monochromator (600 grooves/mm, 330–900 nm) was used for the emission spectra measurement. The signal was detected with a Hamamatsu H8259-01 photon counting unit. The vacuum in the sample chamber was about 1×10^{-5} mbar. The effect of the experimental setup response on the relative VUV excitation intensities of the samples were corrected by dividing the measured excitation intensities of the samples with the excitation intensities of a reference sample sodium salicylate ($o\text{-C}_6\text{H}_4\text{OHCOONa}$) measured simultaneously in the same excitation conditions [12].

3 Results and discussion

3.1 Powder X-ray diffraction

In order to characterize the phase purity of the samples, X-ray powder diffraction (XRD) measurements were performed for all samples. As for example, the XRD patterns of samples $\text{NaGd}(\text{PO}_3)_4$, $\text{NaEu}_{0.50}\text{Gd}_{0.50}(\text{PO}_3)_4$, and $\text{NaEu}(\text{PO}_3)_4$ were plotted in Fig. 1 indicating that all samples are of single phase and in good agreement with the reported powder patterns in JCPDS standard card numbered

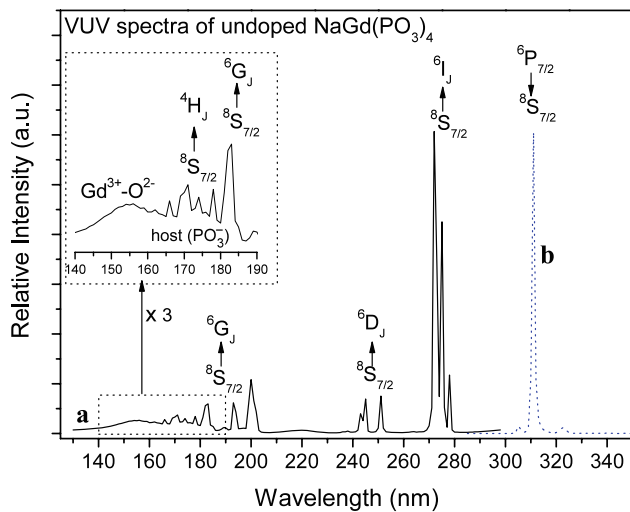


Fig. 2 The VUV spectra of undoped NaGd(PO₃)₄ at RT. **(a)** Excitation spectrum ($\lambda_{em} = 311$ nm), **(b)** emission spectrum ($\lambda_{ex} = 273$ nm)

47-0657 [NaGd(PO₃)₄]. These XRD patterns comparisons also show that the polyphosphate samples were synthesized successfully at 700°C. This calcination temperature is much lower than the preparation temperature (1100°C) of current commercial red-emitting phosphors (Y, Gd)BO₃:Eu³⁺ by the solid-state reaction technique [13], which is in favor of energy saving for our society when the phosphor NaGd(PO₃)₄:Eu³⁺ are synthesized on a large scale as a commercial product.

The compound NaGd(PO₃)₄, crystallizing in a monoclinic system with $P2_1/n$ space group, can be described as a long chain polyphosphate containing alternating zigzag (PO₃)_n chains linked by distorted GdO₈ dodecahedra, and there is only one C₁ site for Gd³⁺ ions which has the lowest symmetry [14]. Because of the much smaller ionic radii difference between rare-earth ions Eu³⁺ (106.6 pm) and Gd³⁺ (105.3 pm) in the eight-fold coordination environment [15], the compound NaEu(PO₃)₄ is isostructure with compound NaGd(PO₃)₄, and the XRD patterns of NaEu_{0.50}Gd_{0.50}(PO₃)₄ and NaEu(PO₃)₄ are the same with that of NaGd(PO₃)₄, although all Gd³⁺ ions were substituted by Eu³⁺ ions in NaEu(PO₃)₄.

3.2 Photon cascade emission of Gd³⁺ in NaGd(PO₃)₄

The VUV excitation spectrum of undoped NaGd(PO₃)₄ by monitoring Gd³⁺ emission at 311 nm (due to the ⁶P_{7/2} → ⁸S_{7/2} transition) is shown as a curve a in Fig. 2. The sharp excitation peaks at around 273, 245, and 201 nm are assigned to the transitions from ground state ⁸S_{7/2} to excited states ⁶I_J, ⁶D_J, and ⁶G_J within Gd³⁺ ion, respectively. And those weak peaks from 162 to 180 nm can be attributed to ⁸S_{7/2} → ⁶H_J transition within Gd³⁺ ion according to [1]. As indicated by the threefold magnified spectrum shown in

the inset of Fig. 2, the broad absorption appearing at 155 nm is ascribed to Gd³⁺-O²⁻ charge transfer transition [3]. And the weak broad band from 165 to 185 nm, which overlaps with the peaks of ⁸S_{7/2} → ⁶H_J transition within Gd³⁺ ion, is considered to be the PO₃⁻ host-lattice-related absorption. In most phosphates, the host absorption of PO₄³⁻ locates at around 170 nm [16] although the structure of NaGd(PO₃)₄ consists of GdO₈ polyhedra sharing oxygen atoms with phosphoric group PO₄, the intrinsic absorption of PO₃⁻ is also considered to be around this wavelength.

Within Gd³⁺ ion, the energy gap between the ⁶G_{7/2} level and the next lower ⁶D_J level is large, so the multiphonon-relaxation rates will be negligibly low. Therefore the photon cascade emission can occur when Gd³⁺ ion is excited to ⁶G_J level. In Gd³⁺ activated fluoride LiYF₄, it was observed that a Gd³⁺ ion excited in the ⁶G_J level can return to the ground state by emitting two photons [1]. But comparing the technique for synthesizing oxide phosphors, the conditions for preparing the fluorides are more fastidious, and the oxide phosphors have higher VUV absorption efficiency [17]. If the quantum cutting of Gd³⁺ ion can occur in oxide phosphors, the Gd³⁺-based compounds could have higher visible quantum efficiency than VUV exciting phosphors.

Figure 3 shows the emission spectrum of undoped NaGd(PO₃)₄ under ⁸S_{7/2} → ⁶G_J excitation (201 nm) at RT. Besides the ultraviolet emission at around 311 nm due to the ⁶P_J → ⁸S_{7/2} transition, there are some weak peaks at around 593 nm. All emission lines in these spectra are assigned to ⁶G_J → ⁶P_J transition of Gd³⁺ ions, whose energy agree very well with the calculated differences between the energies of ⁶G_J levels and the energies of the ⁶P_J levels. The detailed assignments were marked in the magnified ⁶G_J → ⁶P_J emission spectrum shown in the inset of Fig. 3. The fact that Gd³⁺ ion in NaGd(PO₃)₄ excited by ⁸S_{7/2} → ⁶G_J transition emits a red photon due to the ⁶G_J → ⁶P_J transition and an ultraviolet photon due to the ⁶P_J → ⁸S_{7/2} transition, as shown in the left part of Fig. 4, confirms the occurrence of the photon cascade emission of Gd³⁺ in this oxide host lattice polyphosphate NaGd(PO₃)₄.

3.3 Intensive red emission of Eu³⁺ doped in NaGd(PO₃)₄

The emission of Eu³⁺ ion consists usually of lines in the red spectral area, which has important application in lighting and color display. In order to obtain a new red-emitting phosphor, Eu³⁺ ions were doped in the host NaGd(PO₃)₄ by conventional solid-state reactions.

Figure 5 shows the VUV excitation and emission spectra of NaEu_{0.10}Gd_{0.90}(PO₃)₄ at RT, and the VUV spectra of commercial phosphor (Y, Gd)BO₃:Eu³⁺ as a reference were also plotted in this figure. For these curves all parameters were normalized, which include (emission and excitation) slit width, integrated time, beam intensity, and relative intensity of energy at the excitation wavelength.

Fig. 3 Emission spectrum of undoped NaGd(PO₃)₄ under ⁸S_{7/2} → ⁶G_J excitation (201 nm) at RT (the inset figure is the magnified ⁶G_J → ⁶P_J emission spectrum)

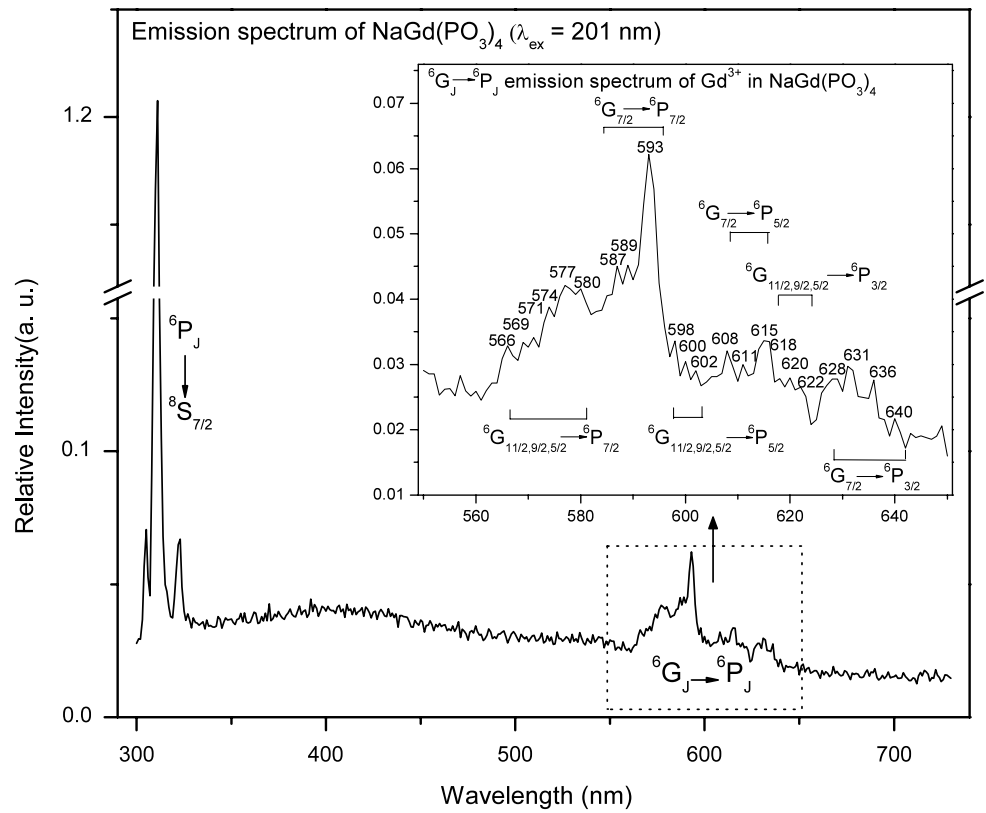
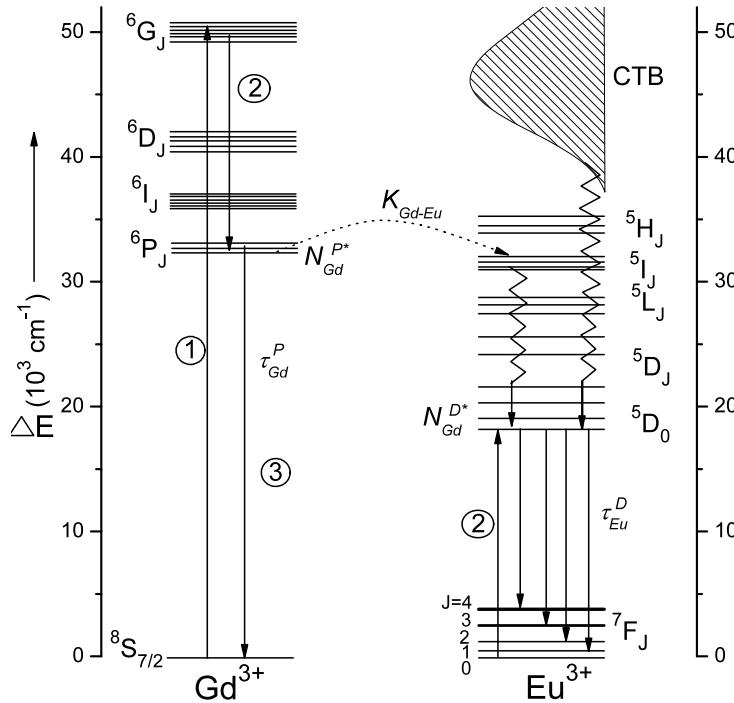


Fig. 4 The transitions for the photon cascade emission of Gd³⁺ ion in undoped NaGd(PO₃)₄ compound and energy transfer from Gd³⁺ to Eu³⁺ ion in NaGd(PO₃)₄:Eu³⁺



The excitation spectra of both red phosphors were measured by monitoring Eu³⁺ emission at 611 nm due to the ⁵D₀ → ⁷F₂ transition. Comparing the excitation spectra of Eu³⁺ ions doped in the host NaGd(PO₃)₄ and (Y, Gd)BO₃,

it can be seen that the maximum of charge transfer band (CTB) of Eu³⁺-O²⁻ in NaGd(PO₃)₄:Eu³⁺ is shifted about 18 nm toward high-energy region, which maybe benefit for the luminescence of NaGd(PO₃)₄:Eu³⁺ under VUV excita-

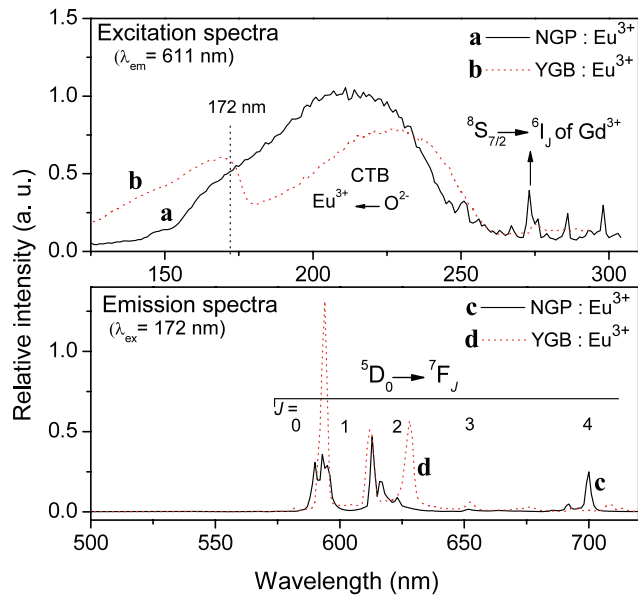


Fig. 5 VUV spectra of $\text{NaEu}_{0.10}\text{Gd}_{0.90}(\text{PO}_3)_4$ (labeled as $\text{NGP}:\text{Eu}^{3+}$) and commercial phosphor $(\text{Y}, \text{Gd})\text{BO}_3:\text{Eu}^{3+}$ ($\text{YGB}:\text{Eu}^{3+}$) at RT

tion because it was concluded by G. Blasse that the luminescence efficiency of phosphors doped Eu^{3+} ions increase with energy increasing of CTB ($\text{Eu}^{3+}-\text{O}^{2-}$) [18].

From the excitation spectra in Fig. 5 it can be observed that both red-emitting phosphors have almost the same absorption intensity at 172 nm, which suggests that $\text{NaGd}(\text{PO}_3)_4:\text{Eu}^{3+}$ could be a potential red-emitting VUV phosphor for mercury-free fluorescent lamps and PDPs applications. Then the emission spectra of $\text{NaGd}(\text{PO}_3)_4:\text{Eu}^{3+}$ and $(\text{Y}, \text{Gd})\text{BO}_3:\text{Eu}^{3+}$ were measured under the 172-nm VUV excitation and both spectra are plotted in Fig. 5 as curves c and d, respectively. The obvious discrepancy between both curves is that the electronic dipole ${}^5\text{D}_0 \rightarrow {}^7\text{F}_2$ transition at 611 nm within $\text{NaGd}(\text{PO}_3)_4:\text{Eu}^{3+}$ is stronger than the emission of magnetic ${}^5\text{D}_0 \rightarrow {}^7\text{F}_1$ transition at 593 nm because of the noninversion symmetry of Eu^{3+} sites in $\text{NaGd}(\text{PO}_3)_4$, while in $(\text{Y}, \text{Gd})\text{BO}_3:\text{Eu}^{3+}$ the later emission is much stronger which results in not having deep red emission [19].

3.4 Energy transfer from Gd^{3+} to Eu^{3+} in $\text{NaGd}(\text{PO}_3)_4:\text{Eu}^{3+}$

$\text{Gd}^{3+}-\text{Eu}^{3+}$ pair was studied sufficiently as efficient energy transfer ion couple by many scientists [20, 21]. In $\text{LiGdF}_4:\text{Eu}^{3+}$ systems a visible quantum efficiency higher than 100% have been obtained through the ${}^6\text{G}_J \rightarrow {}^6\text{P}_J$ (Gd^{3+}) and ${}^7\text{F}_J \rightarrow {}^5\text{D}_0$ (Eu^{3+}) cross-relaxation energy transfer from Gd^{3+} to Eu^{3+} ions [2]. In present study, the emission spectrum of the sample $\text{NaEu}_{0.50}\text{Gd}_{0.50}(\text{PO}_3)_4$ excited by 201 nm vacuum ultraviolet due to ${}^8\text{S}_{7/2} \rightarrow {}^6\text{G}_{7/2}$ transition within Gd^{3+} ion is shown in Fig. 6a. Besides the

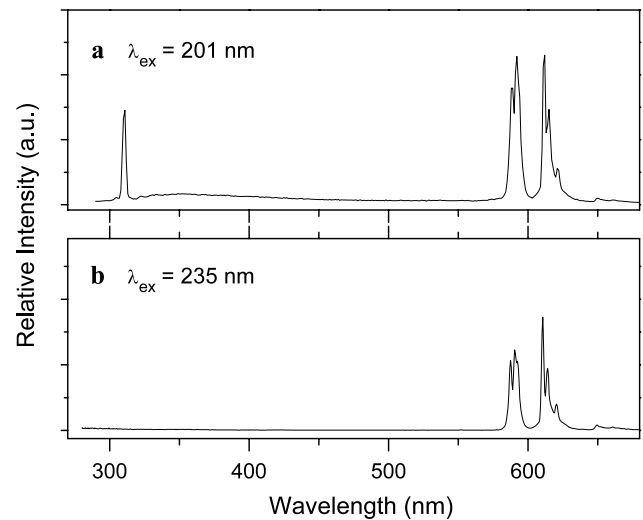


Fig. 6 Emission spectra of $\text{NaGd}_{0.50}\text{Eu}_{0.50}(\text{PO}_3)_4$ at RT

Eu^{3+} red emission due to ${}^5\text{D}_0 \rightarrow {}^7\text{F}_1$ and ${}^5\text{D}_0 \rightarrow {}^7\text{F}_2$ transition, the emission peak of Gd^{3+} ion at around 311 nm due to ${}^6\text{P}_{7/2} \rightarrow {}^8\text{S}_{7/2}$ transition can also be seen. The broad band at around 350 nm is the intrinsic host emission. When the sample $\text{NaEu}_{0.50}\text{Gd}_{0.50}(\text{PO}_3)_4$ was excited by 235-nm ultraviolet due to CTB of $\text{Eu}^{3+}-\text{O}^{2-}$, the characteristic Gd^{3+} ${}^6\text{P}_{7/2} \rightarrow {}^8\text{S}_{7/2}$ emission at 311 nm was insignificant indicating that there is no efficient energy transfer from Eu^{3+} to Gd^{3+} ions in $\text{NaGd}(\text{PO}_3)_4:\text{Eu}^{3+}$, and the energy for Gd^{3+} ultraviolet emission at 311 nm under 201-nm VUV excitation would not come from Eu^{3+} ion although Gd^{3+} and Eu^{3+} have overlap absorption at about 201 nm. Therefore, the photon cascade emission of Gd^{3+} would occur in $\text{NaGd}(\text{PO}_3)_4:\text{Eu}^{3+}$ under VUV excitation and it would improve the red emission of Eu^{3+} through the cross-relaxation energy transfer from Gd^{3+} to Eu^{3+} ions as shown in Fig. 4.

On the other hand, the existence of the emission peak at 311 nm of Gd^{3+} under 201-nm VUV excitation also shows that the energy transfer from Gd^{3+} to Eu^{3+} through energy migration is not complete. In order to investigate the energy transfer behaviors from Gd^{3+} to Eu^{3+} ions in $\text{NaGd}(\text{PO}_3)_4:\text{Eu}^{3+}$, the emission spectra of $\text{NaGd}(\text{PO}_3)_4$ samples doped with different Eu^{3+} concentration were determined under 273-nm UV excitation. As for example, Fig. 7 shows the emission spectra of $\text{NaEu}_x\text{Gd}_{(1-x)}(\text{PO}_3)_4$ samples ($x = 0.1, 0.3, 0.5, 0.7$) in the region between 290 and 680 nm excited at 273 nm corresponding to the ${}^8\text{S}_{7/2} \rightarrow {}^6\text{I}_J$ transition of Gd^{3+} . Both the UV emission of Gd^{3+} at 311 nm and the red emission of Eu^{3+} at 611 nm are observed, and the emission intensity of Gd^{3+} decreases with the increasing Eu^{3+} concentration but does not completely disappear even though the x value in excess of 0.50. The inset figure in Fig. 7 shows the effects of Eu^{3+} addition on the emission intensities of both peaks. It can be concluded that the intensity of Gd^{3+} emission decreases

sharply when Eu^{3+} doping concentration increases from 1.0 to 20.0 mol%, while the intensity of Eu^{3+} emission at 611 nm increases up to 5.0 mol% Eu^{3+} addition and then remains constant till 50.0 mol% Eu^{3+} addition. When the concentration of Eu^{3+} exceeds 60.0 mol%, the intensity of both emission peaks starts to diminish as the absorption for 273-nm UV radiation becomes weak due to the decreasing of Gd^{3+} ions.

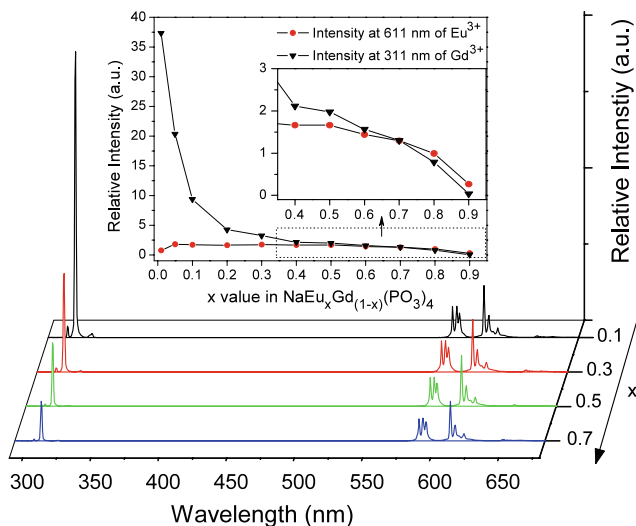


Fig. 7 Emission spectra of $\text{NaEu}_x\text{Gd}_{(1-x)}(\text{PO}_3)_4$ samples under 273-nm UV excitation. The inset figure is the relative emission intensities of peaks at 311 (\blacktriangledown , ${}^6\text{P}_{7/2} \rightarrow {}^8\text{S}_{7/2}$ transition of Gd^{3+}) and 611 nm (\bullet , ${}^5\text{D}_0 \rightarrow {}^7\text{F}_2$ transition of Eu^{3+}) varied with the x value in $\text{NaEu}_x\text{Gd}_{(1-x)}(\text{PO}_3)_4$ samples

Fig. 8 Emission spectra of $\text{NaEu}_x\text{Gd}_{(1-x)}(\text{PO}_3)_4$ samples under 393-nm UV excitation. The inset figure is the relative emission intensities of peaks at 611 nm varied with the x value in $\text{NaEu}_x\text{Gd}_{(1-x)}(\text{PO}_3)_4$ samples

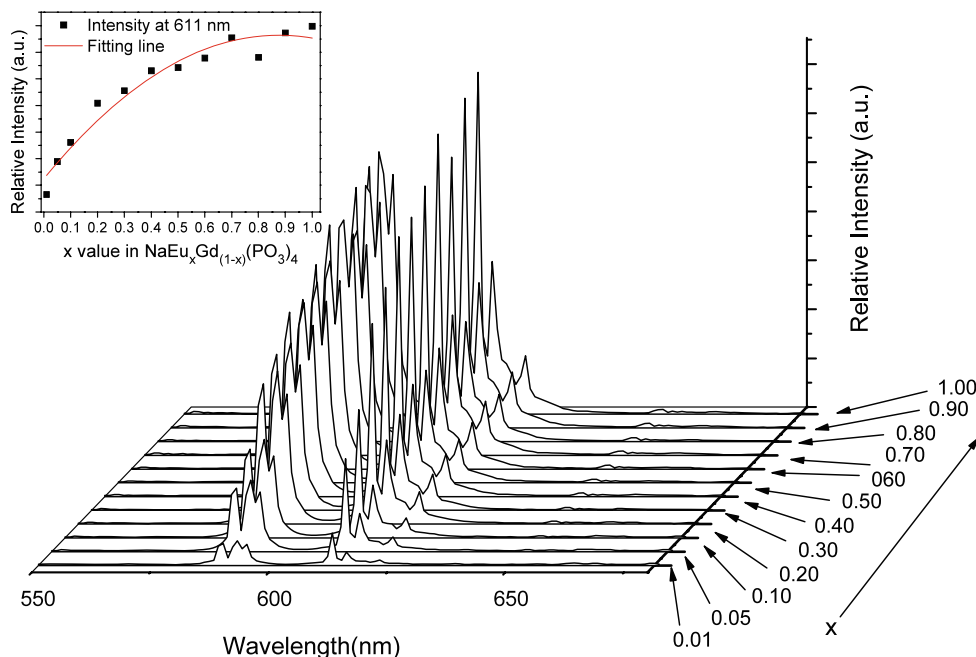


Figure 8 shows Emission spectra of $\text{NaEu}_x\text{Gd}_{(1-x)}(\text{PO}_3)_4$ ($x = 0.01-1.0$) samples in the region between 550 and 680 nm excited at 393 nm corresponding to the ${}^7\text{F}_0 \rightarrow {}^5\text{L}_6$ transition within Eu^{3+} ions. It can be observed that the intensities of Eu^{3+} emission at 611 nm always increase as the growing of Eu^{3+} addition and there is no concentration quenching for the emission of $\text{NaGd}(\text{PO}_3)_4:\text{Eu}^{3+}$ samples even though all Gd^{3+} ions in $\text{NaGd}(\text{PO}_3)_4$ were substituted by Eu^{3+} ions to form the compound $\text{NaEu}(\text{PO}_3)_4$, which means that the energy absorbed directly by Eu^{3+} ions at 393 nm can be effectively converted into the red emission of Eu^{3+} at 611 nm.

These phenomena that the intensities at 611 nm of Eu^{3+} increasing up to a constant under 273-nm UV excitation whereas always increasing under 393-nm UV excitation suggests again that there is energy transfer from Gd^{3+} to Eu^{3+} ions but the energy absorbed by the Gd^{3+} ions at 273 nm can not be transferred completely to Eu^{3+} ions. When the doping concentration of Eu^{3+} was increased up to 5.0 mol%, the efficiency of the energy transfer from Gd^{3+} to Eu^{3+} ions seems to be saturated.

Figure 9 shows the Eu^{3+} ion concentration dependence of the luminescence decay curves of Gd^{3+} emission in $\text{NaEu}_x\text{Gd}_{(1-x)}(\text{PO}_3)_4$ samples under 273-nm UV excitation at RT. All the decay curves can be fitted with the following single-exponential decay equation (1):

$$I(t) = A \exp(-t/\tau_{\text{Gd}}^{\text{P}}), \tag{1}$$

where A is a constant, $\tau_{\text{Gd}}^{\text{P}}$ is the decay time of ${}^6\text{P}_{7/2}$ excited state within Gd^{3+} ion in $\text{NaEu}_x\text{Gd}_{(1-x)}(\text{PO}_3)_4$ samples under 273-nm UV excitation. The fitted results were listed in

Table 1. From the fitted results it can be concluded that the decay rate of the ⁶P_{7/2} state within Gd³⁺ ion under 273-nm UV excitation become faster and faster with the increase of Eu³⁺ concentration.

For simplicity, we assume a quantum efficiency of $\eta = 1$ for Gd³⁺ emission in undoped host NaGd(PO₃)₄. Thus, the energy transfer efficiency (η_{Tr}) from Gd³⁺ to Eu³⁺ in NaEu_xGd_(1-x)(PO₃)₄ samples can be calculated according to the general equation (2) as follows [22]:

$$\eta_{Tr} = 1 - \frac{1/\tau_{Gd_0}^P}{1/\tau_{Gd}^P} = 1 - \frac{\tau_{Gd}^P}{\tau_{Gd_0}^P}, \quad (2)$$

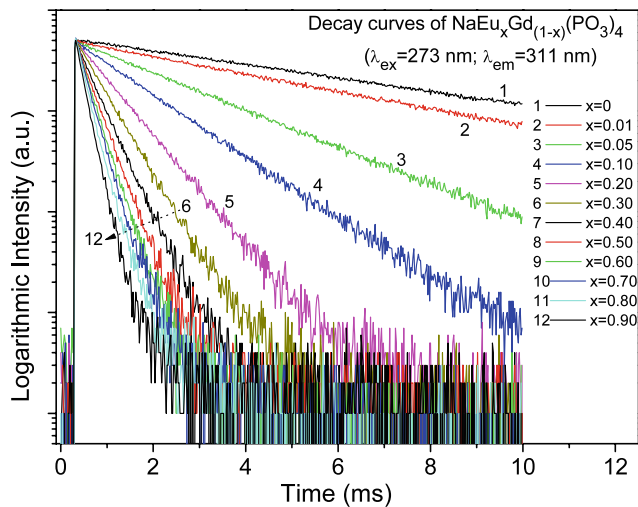
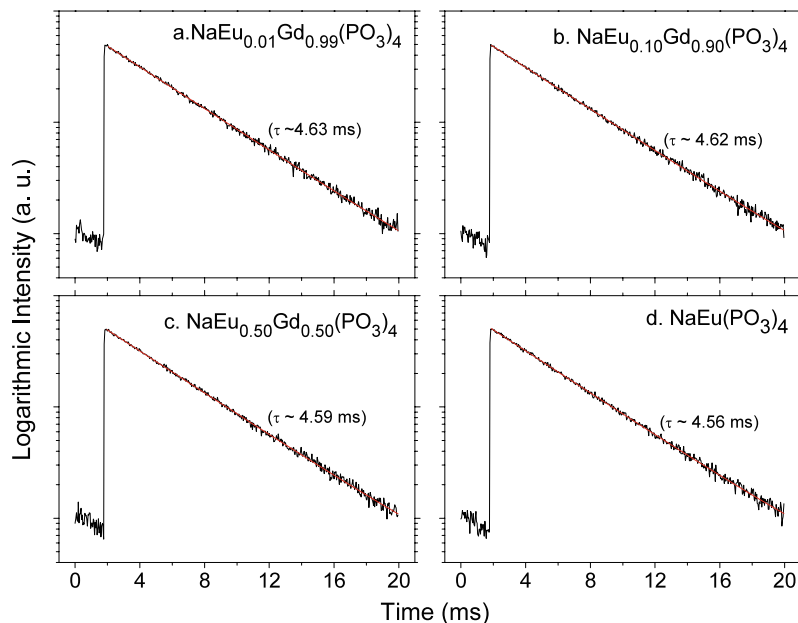


Fig. 9 The Eu³⁺ ion concentration dependence of the luminescence decay curves of Gd³⁺ emission in NaEu_xGd_(1-x)(PO₃)₄ samples under 273-nm UV excitation at RT

Fig. 10 Luminescence decay curves of NaEu_xGd_(1-x)(PO₃)₄ samples ($\lambda_{ex} = 393$ nm, $\lambda_{em} = 611$ nm). All curves were fitted with (1)



where $\tau_{Gd_0}^P$ represents the lifetime value of the ⁶P_{7/2} state within Gd³⁺ in undoped host NaGd(PO₃)₄. All the calculated results of η_{Tr} are also compiled in Table 1.

Figure 10 shows the luminescence decay curves of NaEu_xGd_(1-x)(PO₃)₄ samples when Eu³⁺ ions were directly excited by 393-nm violet light through ⁷F₀ → ⁵L₆ transition within Eu³⁺ ions at RT. All the decay curves also can be fitted with the single-exponential decay equation (1). According to the fitted results, the decay time values for Eu³⁺ transient emission at 611 nm (τ_{Eu}^D) always keep constant at about 4.60 ms as NaEu_xGd_(1-x)(PO₃)₄ samples were excited directly by the ⁷F₀ → ⁵L₆ transition of the

Table 1 The lifetime values of the ⁶P_{7/2} state within Gd³⁺ ions (τ_{Gd}^P) in NaEu_xGd_(1-x)(PO₃)₄ samples under 273-nm UV excitation and the energy transfer efficiency (η_{Tr}) from Gd³⁺ to Eu³⁺

No.	<i>x</i> value	τ_{Gd}^P (ms)	η_{Tr}
1	0	6.36	NA
2	0.01	4.83	0.24
3	0.05	2.34	0.63
4	0.10	1.39	0.78
5	0.20	0.78	0.88
6	0.30	0.55	0.91
7	0.40	0.42	0.93
8	0.50	0.35	0.94
9	0.60	0.30	0.95
10	0.70	0.27	0.96
11	0.80	0.23	0.96
12	0.90	0.20	0.97

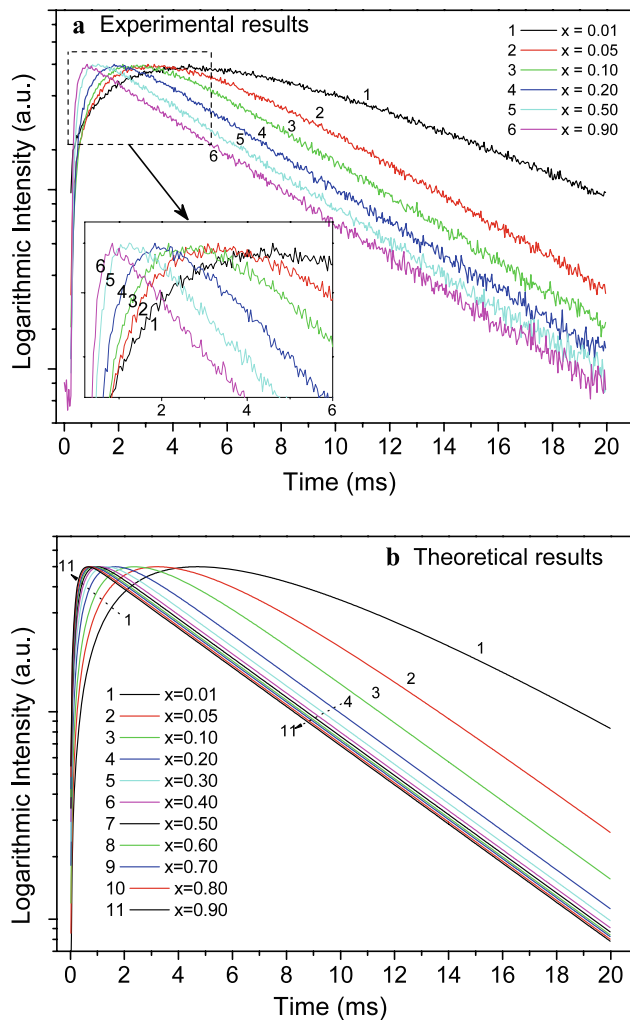


Fig. 11 The Eu^{3+} ion concentration dependence of the luminescence decay curves of $\text{NaEu}_x\text{Gd}_{(1-x)}(\text{PO}_3)_4$ samples at RT ($\lambda_{\text{ex}} = 273$ nm, $\lambda_{\text{em}} = 611$ nm)

Eu^{3+} ions at 393 nm, and this values almost are not influenced by the Eu^{3+} concentrations.

The Eu^{3+} ion concentration dependence of the luminescence decay curves of $\text{NaEu}_x\text{Gd}_{(1-x)}(\text{PO}_3)_4$ samples under 273-nm UV excitation at RT are shown in Fig. 11a. When Gd^{3+} ions were excited by 273-nm UV light, there are two processes in the decay curves for Eu^{3+} emission: build-up process and decay process. Through build-up process, the energies absorbed by the $^8\text{S}_{7/2} \rightarrow ^6\text{I}_{7/2}$ transition within Gd^{3+} ions are transferred to Eu^{3+} ions through energy migration for red emission. From the luminescence decay curves, it can be seen that the build-up process is obviously influenced by the Eu^{3+} concentration, and the build-up processes become faster and faster with the increasing of Eu^{3+} ions (see the magnified figure in Fig. 11a). The decay process varied with Eu^{3+} concentration when the x value in the $\text{NaEu}_x\text{Gd}_{(1-x)}(\text{PO}_3)_4$ is below 0.10, while the decay process do not obviously vary with Eu^{3+} concentration

when x value is above 0.10 and the decay time value reaches about 4.60 ms. This value is the same with the decay time value when Eu^{3+} ions were directly excited by the 393-nm UV (see Fig. 10).

According to the energy transfer from Gd^{3+} to Eu^{3+} ion in $\text{NaGd}(\text{PO}_3)_4:\text{Eu}^{3+}$ as shown in Fig. 4, when $\text{NaEu}_x\text{Gd}_{(1-x)}(\text{PO}_3)_4$ samples were excited by 273-nm UV, the rate equations for the population densities in the excited $^6\text{P}_{7/2}$ state within Gd^{3+} ion and the excited $^5\text{D}_0$ state within Eu^{3+} ion can be expressed as follows:

$$\frac{dN_{\text{Gd}}^{\text{P}*}}{dt} = -\frac{N_{\text{Gd}}^{\text{P}*}}{\tau_{\text{Gd}}^{\text{P}}} - K_{\text{Gd-Eu}}N_{\text{Gd}}^{\text{P}*}, \quad (3)$$

$$\frac{dN_{\text{Eu}}^{\text{D}*}}{dt} = -\frac{N_{\text{Eu}}^{\text{D}*}}{\tau_{\text{Eu}}^{\text{D}}} + K_{\text{Gd-Eu}}N_{\text{Gd}}^{\text{P}*}, \quad (4)$$

where $N_{\text{Gd}}^{\text{P}*}$ and $N_{\text{Eu}}^{\text{D}*}$ are the population densities in the excited $^6\text{P}_{7/2}$ state within Gd^{3+} ion and the excited $^5\text{D}_0$ state within Eu^{3+} ion, respectively, $K_{\text{Gd-Eu}}$ is the nonradiative energy transfer rate from $^6\text{P}_{7/2}$ state of Gd^{3+} to $^5\text{D}_0$ state of Eu^{3+} ions in $\text{NaEu}_x\text{Gd}_{(1-x)}(\text{PO}_3)_4$ samples including the energy migration rate from $^6\text{P}_{7/2}$ state of Gd^{3+} to $^5\text{I}_1$ state of Eu^{3+} ion and the nonradiative relaxation rate from $^5\text{I}_1$ state to $^5\text{D}_0$ state within Eu^{3+} ion. Hence the fluorescence intensity $I(t)$ of Eu^{3+} ions at 611 nm under 273-nm UV excitation can be given by

$$I(t) = N_{\text{Eu}}^{\text{D}*}(t) = \frac{K_{\text{Gd-Eu}}N_{\text{Gd}}^{\text{P}*}(0)}{\left(\frac{1}{\tau_{\text{Eu}}^{\text{D}}} - \frac{1}{\tau_{\text{Gd}}^{\text{P}}}\right)} \left[\exp\left(-\frac{t}{\tau_{\text{Gd}}^{\text{P}}}\right) - \exp\left(-\frac{t}{\tau_{\text{Eu}}^{\text{D}}}\right) \right], \quad (5)$$

where $N_{\text{Gd}}^{\text{P}*}(0)$ is the initial value of the population density in the excited $^6\text{P}_{7/2}$ state within Gd^{3+} ion immediately after the excitation and the nonradiative energy transfer from $^6\text{I}_1$ to $^6\text{P}_1$ state within Gd^{3+} is assumed to be instantaneous.

Using the lifetime values of the $^6\text{P}_{7/2}$ state within Gd^{3+} ion shown in Table 1 and the lifetime value of the $^5\text{D}_0$ state within Eu^{3+} ion fitted from the decay curves in Fig. 10, the simulation results with (5) for the decay curves of Eu^{3+} red emission at 611 nm under 273-nm UV excitation are plotted in Fig. 11b. The theoretical results show a similar trend to that of the experimental observations.

4 Conclusions

The luminescence properties of $\text{NaEu}_x\text{Gd}_{(1-x)}(\text{PO}_3)_4$ samples under VUV excitation and energy transfer processes from Gd^{3+} to Eu^{3+} ions under 273-nm UV excitation were studied. The photon cascade emission of Gd^{3+} in oxide type host $\text{NaGd}(\text{PO}_3)_4$ under $^8\text{S}_{7/2} \rightarrow ^6\text{G}_J$ excitation (201 nm) was observed, and this quantum cutting can improve the

red emission of Eu³⁺ ions by a cross-relaxation energy transfer from Gd³⁺ to Eu³⁺ within NaGd(PO₃)₄:Eu³⁺. Compared with the VUV spectra of commercial phosphor (Y, Gd)BO₃:Eu³⁺, the sample NaEu_{0.10}Gd_{0.90}(PO₃)₄ shows intensive and deeper red emission under 172-nm VUV excitation, so this new red-emitting phosphor NaGd(PO₃)₄:Eu³⁺ has potential applications in PDPs and mercury-free fluorescent lamps considering its lower calcination temperature and high chemical stability at ambient conditions. According to the spectroscopic characteristics and the luminescence decay properties of NaGd(PO₃)₄:Eu³⁺, the Eu³⁺ ion concentration dependence of the luminescence decay curves of emission Eu³⁺ in NaEu_xGd_(1-x)(PO₃)₄ samples under ⁸S_{7/2} → ⁶I_{7/2} excitation (273 nm) within Gd³⁺ ions were simulated with the energy transfer theory, and it was confirmed that the energy absorbed by Gd³⁺ ions cannot be completely transferred to Eu³⁺ ions through the energy migration for Eu³⁺ red emission in NaGd(PO₃)₄:Eu³⁺ system.

Acknowledgements This work was financially supported by the National Basic Research Program of China (973 Program, 2007CB935502), National Natural Science Foundation of China (Grant Nos. 20571088 and 20871121), and China Postdoctoral Science Foundation Funded Project (No. 20080440804).

References

1. R.T. Wegh, H. Donker, A. Meijerink, R.J. Lamminmäki, J. Hölsä, Phys. Rev. B **56**, 13841 (1997)
2. R.T. Wegh, H. Donker, K.D. Oskam, A. Meijerink, Science **283**, 663 (1999)
3. C. Feldmann, T. Jüstel, C.R. Ronda, D.U. Wiechert, J. Lumin. **92**, 245 (2001)
4. H.Y.P. Hong, Mater. Res. Bull. **10**, 635 (1975)
5. K. Jaouadi, H. Naili, N. Zouari, T. Mhiri, A. Daoud, J. Alloys Compd. **354**, 104 (2003)
6. K. Jaouadi, N. Zouari, T. Mhiri, M. Pierrot, J. Cryst. Growth **273**, 638 (2005)
7. H. Ettis, H. Naili, T. Mhiri, Cryst. Growth Des. **3**, 599 (2003)
8. I. Parreu, R. Solé, J. Gavalda, J. Massons, F. Díaz, M. Aguiló, Chem. Mater. **17**, 822 (2005)
9. I. Parreu, J.M.C. Pujol, M. Aguiló, F. Díaz, X. Mateos, V. Petrov, Opt. Express **15**, 2360 (2007)
10. J. Zhong, H. Liang, B. Han, Z. Tian, Q. Su, Y. Tao, Opt. Express **16**, 7508 (2008)
11. J. Zhong, H. Liang, B. Han, Q. Su, Y. Tao, Chem. Phys. Lett. **453**, 192 (2008)
12. J.A.R. Samson, *Techniques of Vacuum Ultraviolet Spectroscopy* (Wiley, New York, 1967)
13. X. Zeng, S. Im, S. Jang, Y. Kim, H. Park, S. Son, H. Hatanaka, G. Kim, S. Kim, J. Lumin. **121**, 1 (2006)
14. J. Amami, M. Ferid, M. Trabelsi-Ayedi, Mater. Res. Bull. **40**, 2144 (2005)
15. R.D. Shannon, Acta Cryst. A **32**, 751 (1976)
16. S.P. Feofilov, Y. Zhou, H.J. Seo, J.Y. Jeong, D.A. Keszler, R.S. Meltzer, Phys. Rev. B **74**, 085101 (2006)
17. K. Toda, J. Alloys Compd. **408**, 665 (2006)
18. G. Blasse, J. Chem. Phys. **45**, 2356 (1966)
19. C.R. Ronda, *Luminescence: From Theory to Applications* (Wiley-VCH, Weinheim, 2008)
20. W. Ryba-Romanowski, S. Golab, G. Dominiak-Dzik, P. Solarz, Appl. Phys. A **74**, 581 (2002)
21. N. Takeuchi, S. Ishida, A. Matsumura, Y. Ishikawa, J. Phys. Chem. B **108**, 12397 (2004)
22. J. García Solé, L.E. Bausá, D. Jaque, *An Introduction to the Optical Spectroscopy of Inorganic Solids* (Wiley, West Sussex, 2005)